

The spatial resolution of a laser interferometer with a pixelated phase mask is found to extend virtually to the limit of the detector.

Pixelated Mask Extends Spatial Resolution

Introduction

In a typical interferometric measurement the primary concern is the ability of an instrument to correctly report the surface height variation of the test object. Figure 1A shows a simulated object surface profile. This profile has a sinusoidal shape of increasing frequency from left to right. An example measurement of the object surface profile is shown in Figure 1B. In this example, the measurement profile accurately reports the sinusoidal surface height only for the very low spatial frequencies at the left of the object. The measured surface height falls as the spatial frequency increases. This fall-off is characteristic of all interferometers and will be determined by the optical resolution of the imaging optics, the size of the detector pixels, and the algorithms used to process the data.

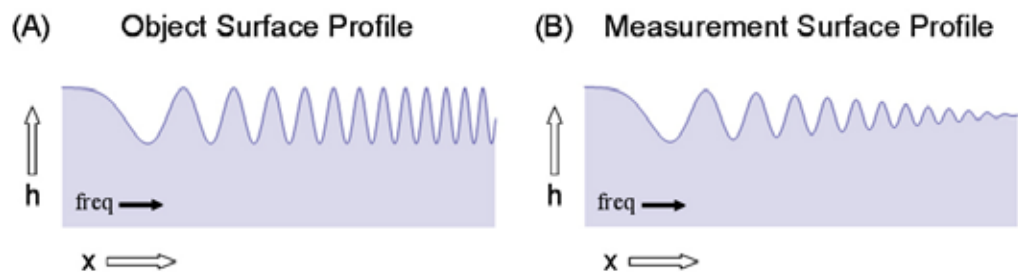


Figure 1. Sinusoidal object surface profile with corresponding measurement surface profile (left). As the spatial frequency of the surface height variation increases, the measured surface height decreases (right).

The instrument transfer function (ITF) is used to describe a system's response in terms of the input signal's frequency content. For an interferometric system measuring surface height, the ITF describes the ratio between the object and image surface height amplitudes for a given spatial frequency. Since an interferometer determines the object height based on a measured phase value, the ITF is sometimes referred to as a Phase Transfer Function.

For the example shown in Figure 1, the object surface height amplitude as a function of frequency is constant. Therefore, the image surface height roll-off with spatial frequency directly corresponds to the ITF of the measurement. This relationship is shown in Figure 2.

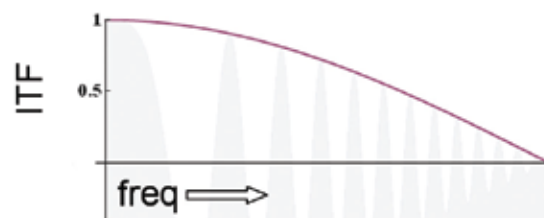


Figure 2. Instrument transfer function derived from the simulated measurement of Figure 1.

Factors Affecting the Instrument Transfer Function

The primary factors affecting the ability of an interferometer to accurately determine the phase profile of the object under test are: 1) the illumination source's spatial and spectral characteristics, 2) the imaging system, 3) the detector sampling, and 4) the phase calculation technique.

Imaging

The initial process in making an interferometric measurement is to image the test and reference wavefronts at the detector. The system numerical aperture, NA, determines the maximum spatial frequency that will pass through the system. For coherent imaging with monochromatic point source illumination, the cut-off frequency is given by NA/λ , where λ is the wavelength of light. Any frequency content beyond the cut-off is blocked and will not contribute to the interferogram, which is subsequently analyzed to determine the phase of the wavefront.

Additionally, due to system aberrations, the frequency cutoff may not be sharp but may gradually roll off towards the cut-off. This will result in an attenuation of the higher frequency content which will affect the interferogram and subsequently the measured phase.

Detector Sampling

A detector with adequate sampling must be used to prevent aliasing of the high spatial frequency content in the interferogram. It is generally adequate to sample at the Nyquist limit which is determined by the image-side NA. Sampling beyond the spatial frequency cutoff provides no additional benefit in terms of system resolution.

Phase Calculation Technique

Phase determination for the pixelated mask sensor utilizes a form of the spatial carrier technique, in which a spatially dependent carrier phase is added to the test and reference wavefronts. The interferogram formed at the detector can be represented as follows:

$$I(x,y) = I_{avg}(x,y)(1 + v \cos[\theta(x,y) + \phi(x,y)]) \tag{2.1}$$

where v is the fringe visibility, $\theta(x,y)$ is the wavefront phase to be determined, and $\phi(x,y)$ is the carrier phase introduced by the pixelated mask. In order to determine the phase, $\theta(x,y)$ from the intensity values given above, two different heterodyne signals are formed by multiplying the intensity values of Equation 2.1 by the sine and cosine of the carrier phase. The results of this multiplication are as follows:

$$I(x,y) \sin[\phi(x,y)] = -\frac{1}{2} I_{avg}(x,y) v \sin[\theta(x,y)] + \frac{1}{2} I_{avg}(x,y) v (\sin[\theta(x,y) + 2\phi(x,y)]) \tag{2.2}$$

$$I(x,y) \cos[\phi(x,y)] = +\frac{1}{2} I_{avg}(x,y) v \cos[\theta(x,y)] + \frac{1}{2} I_{avg}(x,y) v (\cos[\theta(x,y) + 2\phi(x,y)]) \tag{2.3}$$

Notice that the final term in Equations 2.2 and 2.3 is directly proportional to the sine and cosine of the measurement phase. All other terms are modulated by the spatial carrier phase or twice the spatial carrier phase.

In order to recover the $\sin[\theta(x,y)]$ and $\cos[\theta(x,y)]$ terms, the intensity values given in Equations 2.2 and 2.3 must be low pass filtered. Low pass filtering is conducted by convolving the intensity values with a 2x2 or a 3x3 filter as shown in Equation 2.4.

$$I(x,y) \cos[\theta(x,y)] * K_f = \frac{1}{2} I_{avg}(x,y) v \cos[\theta(x,y)]$$

$$I(x,y) \sin[\theta(x,y)] * K_f = -\frac{1}{2} I_{avg}(x,y) v \sin[\theta(x,y)] \tag{2.4}$$

where K_f is the low pass filter convolution kernel. Note that the equalities shown in the above equations are approximate since the low pass filtering operation will necessarily result in an attenuation of the higher spatial frequency information due to the filter function roll-off. The filter kernels and associated filter functions are shown below in Figure 3.

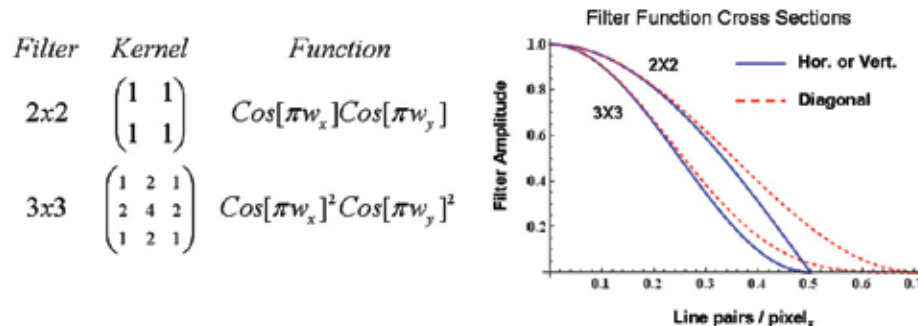


Figure 3. Filter kernels and associated filter functions used in the pixelated mask spatial carrier phase calculation.

where (w_x, w_y) are the spatial frequency coordinates in the x and y directions respectively.

From the above filter function plots we see that the 2x2 kernel has better high frequency performance due to a steeper roll-off. However, note that the 2x2 filter has a very sharp slope at the Nyquist point (0.5 lp/px), whereas the 3x3 filter has a broader area of attenuation at this point. The filter must remove the DC term from the interferogram at this point. If the illumination intensity is not uniform, then the DC term, $I_{avg}(x,y)$, can have a significant spectral width. In this case the 3x3 filter would be a better choice for attenuating this term, preventing it from introducing high frequency noise into the phase calculation.

The final step in determining the phase is to take the arctangent of the ratio of the filtering convolutions shown in Equation 2.4. This process is represented in Equation 2.5 below:

$$\theta(x,y)_c = \text{ArcTan} \left[\frac{\frac{1}{2}I_{avg}(x,y)v\text{Sin}[\theta(x,y)]}{\frac{1}{2}I_{avg}(x,y)v\text{Cos}[\theta(x,y)]} \right] = \text{ArcTan} \left[\frac{\text{Sin}[\theta(x,y)]}{\text{Cos}[\theta(x,y)]} \right] \quad (2.5)$$

where $\theta(x,y)_c$ designates the calculated phase which differs from the actual phase at higher spatial frequencies due to the filtering discussed above.

Effect of the Pixelated Mask Sensor and Algorithms on the ITF

To determine the effect of the pixelated mask sensor and associated algorithms on the ITF, a simulated step height measurement was performed. The simulation assumed a step height of 0.2 waves oriented along the y-axis. The imaging was strictly coherent with the system NA set to produce a cutoff frequency of $\frac{1}{2}$ wave per pixel at the camera. The system is assumed to be diffraction limited. The camera sensor was simulated by an array of 1000 x 1000 pixels with 100% fill factor (i.e., no gaps between the pixels).

These calculations show that using the convolution technique with the pixelated sensor preserves a significant portion of the spatial frequency spectrum. In this example, for a 1000 x 1000 array, the curve labeled “temporal” is the maximum resolution that can be achieved, assuming a diffraction limited optical system and pixels with 100% fill factor. The curve labeled “500 x 500” represents the frequency response that would be achieved for an array with $\frac{1}{4}$ the number of pixels that are twice as wide (equal to 4 pixels of the 1000 x 1000 sensor). For the pixelated phase sensor, the 500 x 500 curve represents the resolution that would be achieved if the array was subdivided into unique groups of 4 neighboring pixels, and a single phase value was calculated for each sub-group. Utilizing the convolution algorithm extends the frequency response out to the limit of the full sensor resolution, significantly beyond the 500 x 500 limit.

Also shown for comparison in Figure 4 is the response of a phase measurement utilizing the spatial carrier method. 100 fringes of linear tilt are used to generate the carrier frequency on a 1000 x 1000 sensor. In this case, the ITF is significantly limited by the frequency response of the Fourier Transform filter.

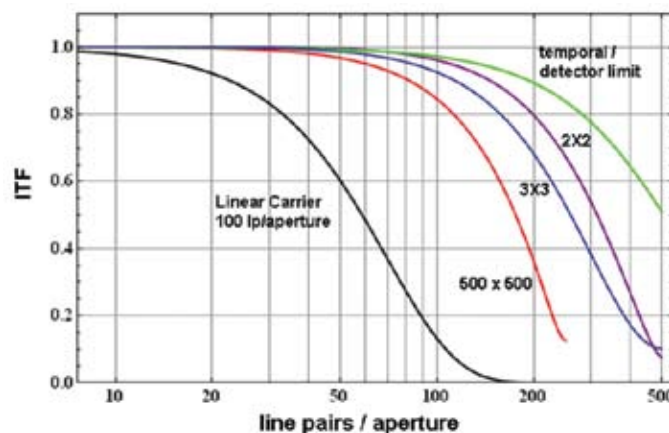


Figure 4. Simulated algorithm effect on ITF for 1k x 1k sensor. The calculation is based on a simulated 0.2 wave step measurement. The camera sensor is a 1000 x 1000 array of square pixels. Various other curves, described in the text, are shown for comparison.

Step Height Measurement ITF Calculation for the 4D FizCam 2000

In order to verify the results of the simulation in section three, the ITF of a 4D Technology FizCam2000 Fizeau interferometer was determined by measuring a 0.2 wave step height standard. The imaging in the FizCam2000 is strictly coherent. The step standard is formed on a 1 inch optical flat and has uniform reflectivity on each side of the step. As in the simulation above, the step was oriented along the y-axis. The calculated ITF along with the corresponding simulated ITF curve is shown in Figure 5. This measurement confirms that the instrument ITF follows the theoretical response.

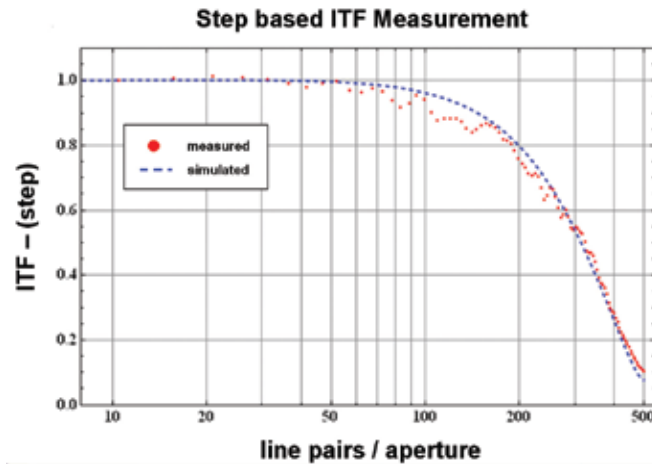


Figure 5. Instrument transfer function for the 4D Technology Fizcam 2000 using the 2 x 2 algorithm. The calculation is based on a 0.2 step height measurement. The Nyquist system aperture size is 100mm. The ITF of the 2 x 2 simulated step height measurement is shown for comparison.

Conclusion

The spatial frequency response of the pixelated phasemask sensor has been investigated both theoretically and experimentally. To achieve optimum performance it is important that the bandwidth of the optical imaging system is adequate so that the limiting factor is the detector pixel width. Actual measurements on a production Fizeau interferometer agree very well with the theory, and demonstrate detector-limited performance. The spatial resolution of the calculated phase map is algorithm dependent; however, both the 2 x 2 and 3 x 3 convolution algorithms result in a frequency response that is significantly more than what would be obtained by a simple parsing of the image. A 1000 x 1000 sensor has a spatial frequency response that is approximately equal to the detector limited resolution of a 700 x 700 array; however, it does have a response that extends to the full Nyquist limit of the 1000 x 1000 array.